Journal of Advanced Electrochemistry 2(2) (2016) 78–84

ISSN: 2455-0205

Contents List available at JACS Directory

Journal of Advanced Electrochemistry

journal homepage: http://www.jacsdirectory.com/jaec

A Green Approach to the Synthesis of Eriochrome Black-T Capped Silver Nanoparticles and Its Electrochemical Detection of L-Tryptophan and L-Tyrosine in Blood Sample and Antibacterial Activity

E. Prabakaran[1], V. Sheela Violet Rani[1], A. Brabakaran[2], K. Pandian[3], D. Jesudurai[1,*]

[1]*Department of Chemistry, GKM College of Engineering & Technology, New Perungalathur, Chennai - 600 063, Tamilnadu, India.*
[2]*CAS in Botany, University of Madras, Guindy Campus, Chennai - 600 025, Tamilnadu, India.*
[3]*Department of Inorganic Chemistry, University of Madras, Guindy Campus, Chennai - 600 025, Tamilnadu, India.*

ARTICLE DETAILS

Article history:
Received 19 April 2016
Accepted 03 May 2016
Available online 18 May 2016

Keywords:
AgNPs@EBT
Electrocatalytic Oxidation
L-Tryptophan
L-Tyrosine
Antibacterial Activity

ABSTRACT

A new development and green approach was adopted for the synthesis of Eriochrome Black-T stabilized silver nanoparticles (AgNPs@EBT) in the presence of sunlight is described. The resulting AgNPs@EBT was isolated and then characterized with Fourier Transform Infrared Spectroscopy (FT-IR), UV-Visible spectroscopy (UV-Vis), Powder X-ray Diffraction Spectroscopy (PXRD) and Field Emission Scanning Electron Microscopy (FE-SEM). The electrochemical behavior of the EBT stabilized silver nanoparticles modified glassy carbon electrode (AgNPs@EBT/GCE) was investigated using a redox probe of $K_3Fe(CN)_6$. The electro-catalytic characteristics of AgNPs@EBT/GCE were used for the electrochemical oxidation of L-Tryptophan (L-Trp) and L-Tyrosine (L-Tyr) in the presence of 0.1 M PBS as supporting electrolyte. The AgNPs@EBT/GCE exhibits high electrocatalytic activity towards the oxidation of both L-Trp and L-Tyr. The AgNPs@EBT/GCE shows a linear response to L-Trp between 0.1×10^{-6} M and 10×10^{-5} M and for L-Tyr, it is between 0.1×10^{-6} M and 0.9×10^{-6} M. The detection limit for L-Trp and L-Tyr is 9.84×10^{-8} M and 9.81×10^{-8} M, respectively. In addition, the modified AgNPs@EBT/GCE displays good sensor activity and making it suitable for the determination of L-Trp and L-Tyr in blood samples. The antibacterial activity of AgNPs@EBT synthesized by the green method was tested against gram negative and gram positive micro-organisms. There is an enhanced antibacterial activity was observed with AgNPs@EBT, when compared with EBT alone.

1. Introduction

The investigation on amino acids receives immense interest as they play major roles in human nervous system, hormone production and muscular structure. Moreover, they are essential for the growth and functioning of various organs and cellular structure [1]. The amino acid L-tryptophan (L-Trp) is widely utilized in medicine as an aid to treat sleep problems (insomnia), anxiety, depression, premenstrual tension and attention deficit disorder. It is also an indispensable amino acid for maintaining nutritional balance in human. Biologically, L-Trp is synthesized from serotonin, epinephrine and norepinephrine, dopamine and melatonin as a precursor and affects the persons, who cannot produce it by metabolic pathway [2]. The minimum dietary dosage of L-Trp is between 0.25 g and 0.15 g and excess of L-Trp causes hepatic disease [3]. When consumed in higher concentration, L-Tyr causes hyperthyroidism in human body and culture medium which induces sister chromatid exchange [4]. The lower consumption of L-Tyr leads to various diseases such as hypochondria, dementia, hypothyroidism, Parkinson's disease and albinism [2]. L-Tyr is also helpful in reducing the stress, cold, fatigue, minimizes sleep and increased wakefulness, reduction of hormones and renal failure [4, 5]. Therefore, it is important to detect the concentration of L-Trp and L-Tyr in various biological fluids. Several electrochemical methods have been extensively employed for the detection of L-Trp and L-Tyr depends on their electrochemical properties at the electrode surface [6]. These amino acids exhibit slow electrochemical response over higher oxidation potential. A considerable number of research works have been done to improve the chemically modified electrodes to enhance the detection of electrochemical sensors for L-Trp and L-Tyr and the sensor capability was compared with other modified glassy carbon electrodes [7-14].

Metal nanoparticles play an important role in fabricating nanoscale devices. The synthesis and characterization of nanoparticles received much attention due to their attractive physical properties and their potential applications in fabricating optoelectric, thermoelectric and magnetic devices [15, 16]. The size and shape of metal nanoparticles are important as they substantially affect the physical and chemical properties such as optical [17], catalysis [18], biological diagnostics [19], antimicrobial [20] and antibacterial activities [21]. Silver nanoparticles incorporated into various matrices have intensively been investigated in order to expand their utility in nanomaterials, biomedical [22] and sensor applications [23].

The synthesis of silver nanoparticles by the reduction of $AgNO_3$ in solution involves two steps such as nucleation and growth [24]. The rate of nucleation and growth of silver nanoparticles decides the dimension of the final products. The dimension of the fine sized silver nanoparticles can be altered by different control parameters such as concentration of reactants, reductant, pH and temperature. Therefore, a number of improved syntheses of nanoparticles could be obtained by changing the parameters like different stabilizing agents and reaction conditions. The silver nanoparticles have also been synthesized by various chemical reduction methods using ascorbic acid, citrate and $NaBH_4$ [25-29]. But, these methods require huge quantity of chemicals and controlling the particle size is difficult. In recent years, these drawbacks have been removed by using sunlight as the source of motivator. Sun light acts as an external motivator to control the size of AgNPs, which would provide sufficient energy to get the particle of required size. In addition, the utilization of sunlight possesses the following advantages: nontoxic nature, nonpolluting and simple in chemical processes. Literatures regarding the synthesis of AgNPs at ambient conditions are reported elsewhere [30, 31].

For the synthesis of nanoparticles, the usage of an organic dye as a stabilizing agent gives improved properties rather than other stabilizing agents such as polymers [32], leaf [33], fruit extracts [34], glucose [35] and carbon materials [28]. Moreover, the dye is a better stabilizing agent than

*Corresponding Author
Email Address: jesuresearch@gmail.com (D. Jesudurai)

2455-0205 / JACS Directory©2016. All Rights Reserved

Cite this Article as: E. Prabakaran, V. Sheela Violet Rani, A. Brabakaran, K. Pandian, D. Jesudurai, A green approach to the synthesis of Eriochrome Black-T capped silver nanoparticles and its electrochemical detection of L-tryptophan and L-tyrosine in blood sample and antibacterial activity, J. Adv. Electrochem. 2(2) (2016) 78–84.

the above mentioned agents because, it has special ionic, polar, non-bonding functional groups (-azo, -sulphite, -hydroxyl and -nitro) and is highly a conjugated л - bonded system [36]. The synthesis of silver nanoparticles by using Alizarin Yellow 2G (AY) as a stabilizing agent with hydrazine as a reducing agent in water and chlorobutane medium has also been described. Similarly, the synthesis of nanoparticles in the macro-emulsion and film like ME-MELLF form is also reported elsewhere [37-39].

In this paper, we present a new development and green approach using 2-hydroxy-1-(1-hydroxy-2-naphthylazo)-6-nitronaphthalene-4-sulfonic acid sodium salt (Eriochrome Black-T, EBT) as a dye and as a stabilizing agent for synthesizing silver nanoparticles. The synthesis of silver nanoparticles by using EBT, when exposed to sunlight without the addition of reducing agent is shown in Scheme1. To our best knowledge, no such reports were found for the synthesis of EBT-capped silver nanoparticles by adopting this green method. UV-Visible spectroscopy was utilized to follow the production of EBT stabilized silver nanoparticles (AgNPs@EBT) by this green method. Furthermore, the AgNPs@EBT modified on GCE (AgNPs@EBT/GCE) was employed for the electrochemical determination of L-Trp and L-Tyr in blood samples. This method is the first one for the electrochemical detection of L-Trp and L-Tyr by using AgNPs@EBT/GCE. The AgNPs@EBT was successfully tested for the antibacterial activity towards human pathogens.

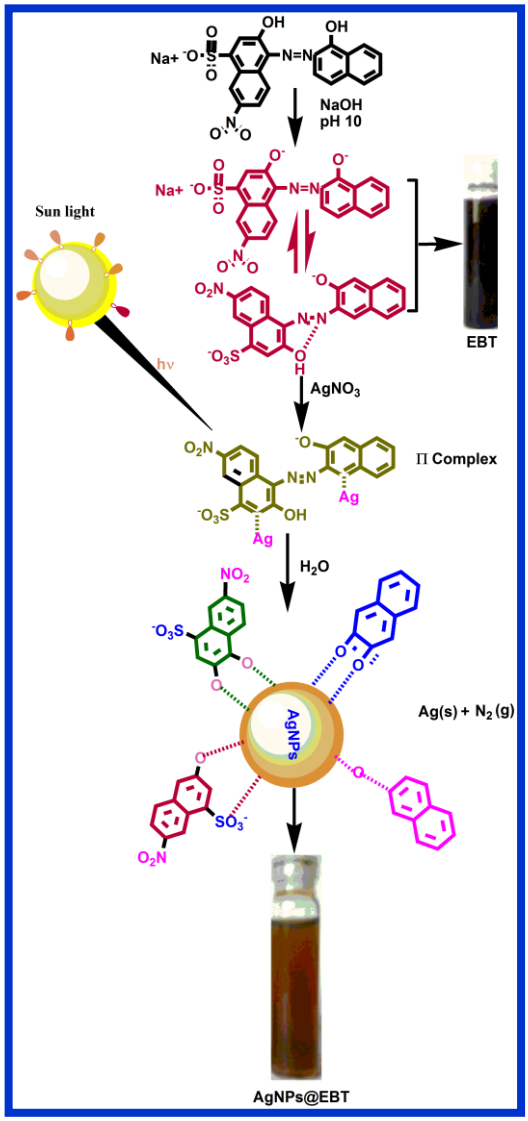

Scheme 1 Synthesis of EBT stabilized AgNPs by green method at pH 10

2. Experimental Methods

2.1 Materials

Silver nitrate ($AgNO_3$, 99.8%), EBT and NaOH were purchased from Merck and the solutions were maintained at pH 10. L-tryptophan and L-tyrosine were obtained from Sigma Aldrich, Bangalore, India and used as received. Anhydrous ethanol (EtOH, 98%) was also purchased from Merck. All chemicals used are of analytical reagents grade. Milli-Q water with resistivity of 18.1 MΩ was used in the experiment and the temperature was controlled at 25 °C.

2.2 Instrumentation

UV-Visible absorption spectra were recorded on a Shimadzu UV-visible spectrophotometer (UV-1800, Japan). The morphology of the sample was observed with Field Emission Scanning Electron Microscopy (FE-SEM) HITACHI Ltd (SU-6600). The X-ray Diffraction (XRD) pattern was taken with a Philips instrument (JSO Debye Flex 2002 Seifert) in the angular range 10^o to 80^o. Fourier Transform Infrared Spectroscopy (FT-IR) spectra were recorded using a Perkin-Elmer, USA (Model Y 40) in the range of 4000 - 400 cm^{-1}. All FT-IR spectra were corrected against the background spectrum of KBr. Electrochemical measurements were conducted using CH600 Instruments, with a single compartment cell setup. The GCE and Pt wire were used as working electrode and counter electrode, respectively. Ag/AgCl was used as reference electrode. The electro-impedance spectroscopy (EIS) measurements were recorded in the frequency range of 0.1 Hz to 100 kHz at 0.24 V. Samples were purged with nitrogen gas for about 10 min before performing all electrochemical experiments.

2.3 Purification of Glassy Carbon Electrode (GCE)

Glassy Carbon electrodes were hand-polished for 3 min on a wet soft polishing cloth with alumina powder of mesh size 0.5 and 0.03 μm and then washed with distilled water. The electrodes were rinsed with water between each step and at the end of polishing. After sonication in absolute ethanol and water for 2 min successively, the mirror-like GCE was dried with purified nitrogen (N_2). The dried GCE was then treated with cyclic scanning in the potential range of 0.2 V to -1.8 V at 0.1 V/s in 0.1 M Phosphate Buffer Saline (PBS pH = 7.0) solution containing 1×10^{-3} M L-Trp and L-Tyr.

2.4 Synthesis of EBT Stabilized AgNPs by Green Method

Silver nanoparticles were synthesized by adopting a green approach using EBT as a stabilizing agent as well as reducing agent. 0.01 g (0.11 mM) of $AgNO_3$ and 0.10 g (0.22 mM) of EBT were dispersed in 25 mL of 0.025 g (0.625 mM) NaOH (pH 10) in a 100 ml beaker with stirring, for about 5 min and then exposed to visible light for 30 min in static condition. The solution colour changes from wine red to brownish yellow colour indicating the formation of silver nanoparticles (Scheme1) [37, 38]. The resultant reaction mixture was then kept at normal room condition and washed with water and ethanol and dried in vacuum desiccator.

2.5 Antibacterial Assay

The antibacterial studies of EBT and AgNPs@EBT were carried out against human pathogenic gram positive *Staphylococcus Aureus and Streptococcus species* and gram negative Escherichia *Coli* and *Klebsilla species* using disc diffusion method [40]. Petri plates were prepared by pouring 10 mL of Mueller Hinton Agar for bacteria and allowed to solidify. These agar plates were inoculated with 0.1 ml of standardized bacterial suspension (2×10^6 cells/mL) and uniformly spread. A 6 mm well was cut at the centre of the agar plate and the well was filled with 10% DMSO of EBT and AgNPs@EBT. The diameter of the inhibition zone observed around the well was measured for each bacterium after 24 hrs of incubation at 37 °C. The well filled with sterile distilled water was served as the control.

3. Results and Discussion

3.1 Green Synthesis of EBT-Capped Silver Nanoparticles (AgNPs@EBT)

The synthesis of AgNPs@EBT stabilized by EBT at pH 10 in the presence of sun light is pictorially represented in Scheme 1 [38]. The AgNPs@EBT was obtained at room temperature when a solution of aqueous $AgNO_3$ in EBT was exposed to sun light. The reaction mixture was kept at room temperature in the presence of sun light for about 30 min. When look at the structure of EBT, it contains a number of active functional groups (-N=N-, -OH, $-SO_3$ and $-NO_2$) in its structure. During the formation of AgNPs@EBT, the AgNPs interact ionically with hydroxyl groups of 2, 3-dihydroxy napthol of EBT. The synthesis of AgNPs in the presence of EBT under different pH of 5, 7, 10 and 12 for 1 h at dark condition is reported elsewhere [39]. In this study, the formation of AgNPs@EBT is occurred within 30 min of time at room temperature in the presence of EBT under a constant pH 10, and exposed to sunlight without the need for any inert atmosphere and reducing agent. The present green method has the following advantages such as: AgNPs@EBT was made by chemical reduction using EBT as a capping agent as well as reducing agent and

Cite this Article as: E. Prabakaran, V. Sheela Violet Rani, A. Brabakaran, K. Pandian, D. Jesudurai, A green approach to the synthesis of Eriochrome Black-T capped silver nanoparticles and its electrochemical detection of L-tryptophan and L-tyrosine in blood sample and antibacterial activity, J. Adv. Electrochem. 2(2) (2016) 78–84.

$AgNO_3$ was used as a salt precursor. Moreover, no additional surfactant or reducing agent was needed for the preparation of AgNPs@EBT. The synthetic approach is a green one that could open a myriad of new nanomaterials.

3.2 Fourier Transform Infrared (FT-IR) Spectral Analysis

In order to ascertain the capping of EBT on silver nanoparticles, the FT-IR spectra of EBT and AgNPs@EBT were analyzed in the range of 400 cm^{-1} to 4000 cm^{-1} and are displayed in Fig. 1(A and B), respectively. In the Fig. 1A, the stretching vibration bands at 3432 cm^{-1}, 1331 cm^{-1}, 1401 cm^{-1} and 1214 cm^{-1} are attributed to -OH, -N=N-, $-NO_2$ and $-SO_3$ groups, respectively. The stretching of -C-O present in the aromatic ring was appeared at 1615 cm^{-1} and the -C=C- stretching appeared in the region 1214 -1183 cm^{-1} and the O-H bending at 964 cm^{-1}. The aromatic -C-H stretching of EBT was found in the region of 2964-2903 cm^{-1} as shown in Fig. 1A. The FT-IR spectrum of AgNPs@EBT shows the following features: The stretching vibration of $-NO_2$, $-SO_3$, -C=C- and -OH bending is shifted to lower wave numbers at 1376 cm^{-1}, 1177 cm^{-1}, 1060 cm^{-1} and 843 cm^{-1}, respectively. The stretching mode of -OH and -C-O is shifted to the higher wave number positions at 3454 cm^{-1} and 1692 cm^{-1}, respectively. The strong interaction between the -OH of EBT and AgNPs is responsible for the shifting of the –OH stretching vibration towards higher wave number, during the formation of AgNPs@EBT. The shifting of peaks to lower wave number is due to the less interaction between the functional groups such as: $-NO_2$ and $-SO_3$ with AgNPs as shown in Fig. 1B [36]. The peak observed at 1331 cm^{-1} corresponding to the stretching of -N=N- moiety of EBT disappeared during the formation of AgNPs@EBT. This observation clearly indicates the oxidation of EBT and the simultaneous reduction of Ag^+ to AgNPs, as displayed in Scheme 1.

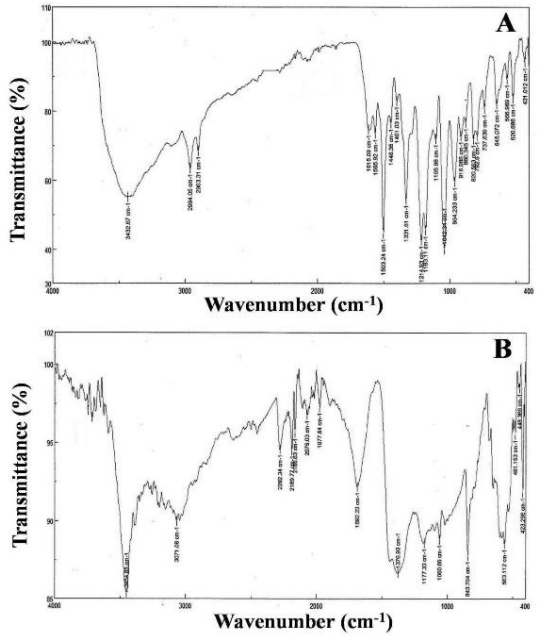

Fig. 1 Fourier transform infrared spectra of (A) EBT and (B) AgNPs@EBT

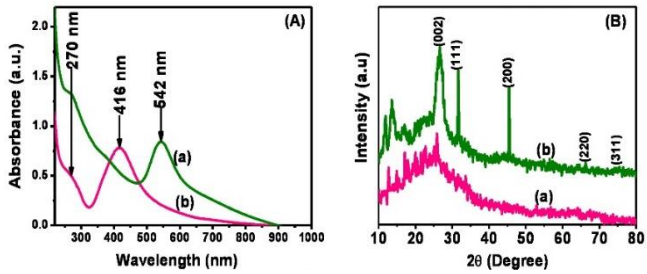

Fig. 2 (A) UV-Visible spectra of (a) EBT and (b) AgNPs@EBT, (B) X-ray diffraction patterns of (a) EBT and (b) AgNPs@EBT.

3.3 UV-Visible Spectral Properties of AgNPs@EBT

The formation of AgNPs@EBT was further confirmed by UV-Visible spectroscopy. The Fig. 2A(a and b) shows the UV-Visible spectra of both EBT and AgNPs@EBT. The absorption spectra of EBT dye solution shows two bands at 542 nm and 270 nm due to -N=N- and OH groups, respectively is shown in Fig. 2A(a) [37]. The formation of AgNPs@EBT was confirmed by the emergence of band at 416 nm, due to the surface plasmon resonance as shown in Fig. 2A(b). As the reaction progresses, there is a continuous decrease in the intensity of band at 542 nm and a simultaneous increase in intensity of band at 416 nm. The interaction between the AgNPs and the EBT through its OH group is responsible for the broadening of peak at 416 nm and the eventual disappearance of peak at 542 nm. This observation is a clear indication of the production of AgNPs@EBT.

3.4 X-Ray Diffraction Characterizations

The XRD patterns observed for EBT and AgNPs@EBT are shown in Fig. 2B(a and b). The peak at 2θ = 26.38° is assigned to (002) lattice plane of semi-crystalline EBT is shown in Fig. 2B(a). The low intensity peak at 2θ = 26.38° increases as the semi-crystalline EBT is converted into crystalline AgNPs@EBT as exemplified from the Fig. 2B(a, b). The other diffraction peaks observed for AgNPs@EBT is assigned to (111), (200), (220) and (311) lattice planes. The obtained peak positions could be well indexed and indicates the FCC structure of the AgNPs@EBT (JCPDS Silver, File -04-0783). In the Fig. 2B(b), the peaks appeared at 2θ = 11.85° and 13.62°, are corresponding to the formation of crystalline EBT (in AgNPs@EBT), when it is converted from amorphous EBT to crystalline AgNPs@EBT [33]. Thus, the XRD patterns give valuable information about the crystalline plane of the face-centered-cubic (FCC) structured Ag^0 and suggesting the crystalline nature of this AgNPs@EBT as shown in Fig. 2B(b).

3.5 FE-SEM Image of AgNPs@EBT

The morphology of silver nanoaprticles coated EBT (AgNPs@EBT) was investigated by using field emission scanning electron microscope (FESEM) and it is depicted in Fig. 3(A-D). The spherical-shaped silver nanoparticles dispersed on EBT with the magnification of 2.00 µm are shown in Fig. 3A. Densely populated spherical-shaped silver nanoparticles are shown at a higher magnification of 1.00 µm and are displayed in Fig. 3B. At a higher magnification of 500 nm, the clear image of spherical-shaped silver nanoparticles are visible and is shown in Fig. 3C. The exact size of the Ag nanoparticles might not be calculated from the SEM images because all silver nanoparticles were obtained in an aggregated form. The chemical composition of AgNPs@EBT was determined by EDAX pattern and the results are shown in Fig. 3D. The major peaks for Ag, Na and O elements were observed in the case of AgNPs@EBT. In addition, a less intense peak was also observed due to glass substrate (Si). All the above FESEM observations indicate the formation of AgNPs@EBT.

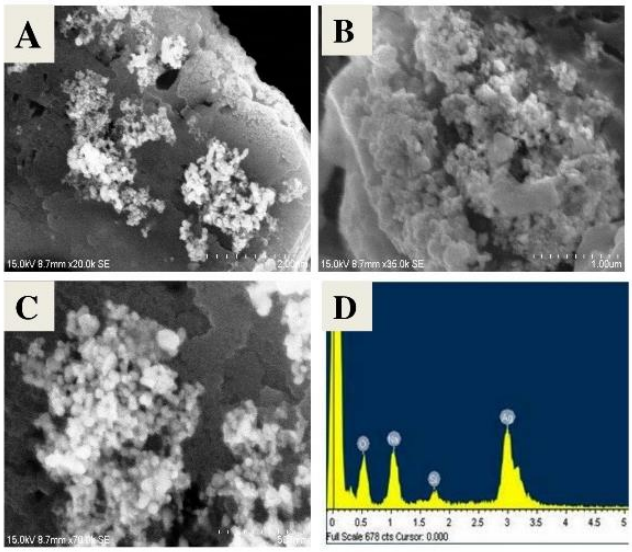

Fig. 3 FESEM image of AgNPs@EBT at different magnification (A) 2.00 µm, (B) 1.00 µm and (C) 500 nm and (D) EDAX pattern of AgNPs@EBT

3.6 Electrode Characterization of Modified AgNPs@EBT/GCE

The CV of the synthesized AgNPs@EBT was carried out by using the ferricyanide system and is found to be a valuable tool for the investigation of kinetic barrier of the interface between the modified electrode and solution. Fig. 4A(c) shows a better redox behaviour due to AgNPs@EBT/GCE than the other two systems such as EBT/GCE (Fig. 4A (b)) and GCE (Fig. 4A(a)) in 5 mM Fe $(CN)_6^{3-/4-}$ and 0.1 M PBS solution. The reversible peak potential distance was calculated using the formula $\Delta Ep = E_{pa}-E_{pc}$ and the values are found to be 269 mV s^{-1}, 294 mV s^{-1} and 246 mV s^{-1} for GCE, EBT/GCE and AgNPs@EBT/GCE, respectively. The peak

Cite this Article as: E. Prabakaran, V. Sheela Violet Rani, A. Brabakaran, K. Pandian, D. Jesudurai, A green approach to the synthesis of Eriochrome Black-T capped silver nanoparticles and its electrochemical detection of L-tryptophan and L-tyrosine in blood sample and antibacterial activity, J. Adv. Electrochem. 2(2) (2016) 78–84.

separation value (ΔEp) on EBT/GCE and AgNPs@EBT/GCE was calculated using Nicholson's theory [41]. Among the three electrode systems, a lower peak separation (ΔEp) value was found in the case of AgNPs@EBT/GCE. This feature explains the fast electron transfer reaction occurred between the electrode of AgNPs@EBT/GCE and the electrolyte solution. The heterogeneous rate constant was calculated using the unmodified GCE, modified EBT/GCE and AgNPs@EBT/GCE and is given in Table 1.

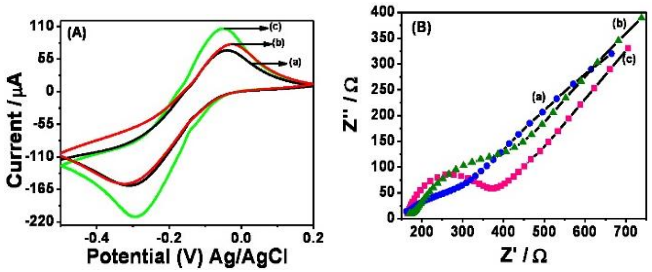

Fig. 4 (A) Electrochemical behavior of the modified electrode at surface modification by CV measurement on GCE (a), EBT/GCE (b) and AgNPs@EBT/GCE (c) with 0.1 M KCl and 5 mM $[K_3Fe(CN)_6]$. Scan rate 50 mV/s. (B) Electrochemical impedance spectra of GCE (a), EBT/GCE (b) and AgNPs@EBT/GCE (c) in 0.1 M KCl containing 5×10^{-3} M $[Fe(CN)_6^{-3/-4}]$ Amplitude: 5 mV.

Table 1 The rate constant of the $Fe(CN)_6^{3-}/Fe(CN)_6^{4-}$ couple in a 0.1 M PBS (pH 6.0) solution containing 1.0 mM $K_4Fe(CN)_6$

Modified electrode	Measurement Method	$\Delta E_p = E_{pa} - E_{pc}$ (mV)	k_s (cm/s)
GCE	CV	269	1.41×10^{-7}
EBT/GCE		294	2.4×10^{-7}
AgNPs@EBT/GCE		246	1.53×10^{-7}

CV: cyclicvoltammetry; k_s values from CV; K_s is the heterogeneous rate constant of the ferricyanide couple in cms^{-1}

The electron transfer behaviour and resistivity were studied about the modified AgNPs@EBT/GCE by EIS technique. The structure characteristic of modified AgNPs@EBT/GCE was analyzed in electrode and in electrolyte solution. The semicircle parameters observed in EIS are due to the following aspects: the electron transfer resistance (R_{et}) and the double layer capacity (C_{dl}) nature of the modified GCE. Fig. 4B(a-c) show the Faradic impedance spectra, presented as Nyquist plots (Z"im vs. Zre) for the bare GCE (a), EBT/GCE (b) and AgNPs@EBT/GCE (c). The bare GCE exhibits almost a straight line pattern (at low frequency) R_{et} = 666.30 (Z'/Ω). This observation indicates the diffusion limited electron-transfer process as shown in Fig. 4B(a). The spectrum of EBT/GCE is nearly a straight line with R_{et} = 738.40 (Z'/Ω), which corresponds to mass diffusion controlled electron transfer process as shown in Fig. 4B(b). The spectrum of AgNPs@EBT/GCE clearly shows the semicircle at R_{et} =705.48 (Z'/Ω. Among the three systems, the AgNPs@EBT/GCE display fast electron transfer process as shown in Fig. 4B(c).

3.7 Electrochemical Oxidation of L-Trp and L-Tyr by AgNPs@EBT/GCE

The AgNPs@EBT/GCE was employed for the electrochemical oxidation of L-Trp and L-Tyr by cyclicvoltammetry and the observed CV is shown in Fig. 5(A-D). The Fig. 5(A-D), illustrate the voltammetry behavior of L-Trp and L-Tyr, recorded at (a) Bare (b) GCE (c) EBT/GCE and (d) AgNPs@EBT/GCE using 0.1 M PBS as supporting electrolyte at (pH 6.0). The GCE and EBT/GCE revealed a lower oxidation peak potential and peak current according to Fig. 5A(b and c). But, the AgNPs@EBT/GCE shows an irreversible oxidation peak potential at E_{pa} of 0.55 V presented in Fig. 5A (d). The CV data furnishes the information that both GCE and EBT/GCE exhibit poor electrochemical oxidation peak current when compared to AgNPs@EBT/GCE on L-Trp system. In the case of L-Tyr, there is a shifting of peak potential (0.488 V) with an increasing peak current when using AgNPs@EBT/GCE system than the GCE and EBT/GCE systems according to Fig. 5B(b-d). The enhancement of peak current and peak potential is observed only in the case of modified AgNPs@EBT/GCE, due to decrease in over potential. This electrode behavior of AgNPs@EBT/GCE is responsible for the easy oxidation of L-Trp and L-Tyr as shown in Fig. 5A (d) and Fig. 5B(d), respectively. Additionally, there is a new low intense peak (Fig. 5A(d)) and a high intense peak (Fig. 5B(d)) are observed with peak potential close to -0.45 V and –0.41 V vs. Ag/AgCl, respectively. This is due to the oxidation of Ag^0/Ag^+ in AgNPs@EBT/GCE, which further evidences the AgNPs coated on EBT. Furthermore, the mechanism of electrochemical oxidation of L-Trp and L-Tyr taking place at AgNPs@EBT/GCE is displayed in Scheme 2.

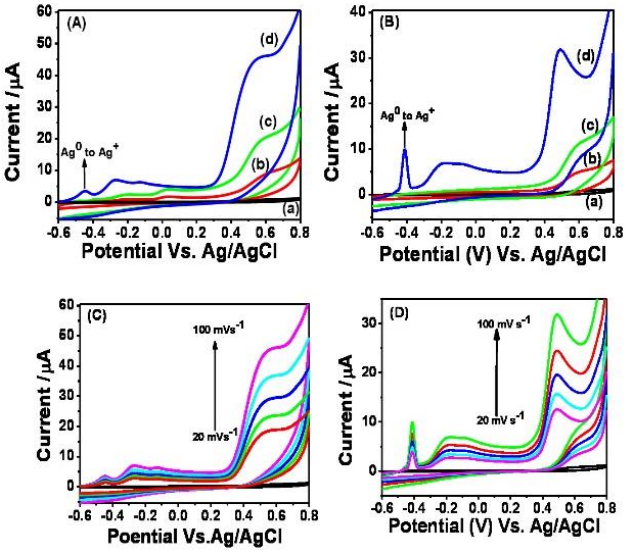

Fig. 5 Cyclicvoltammograms for Bare (a), GCE (b), EBT/GCE (c) and AgNPs@EBT/GCE (d) in 1×10^{-3} M of L-Trp (A) and L-Tyr (B) observed in 0.1 M PBS (pH 6.0) at 100 mVs^{-1} scan rate. CV of 1×10^{-3} M of L-Trp (C) and L-Tyr (D) observed in 0.1 M PBS (pH 6.0) on AgNPs@GO/GCE at different scan rate 20-100 mVs^{-1}.

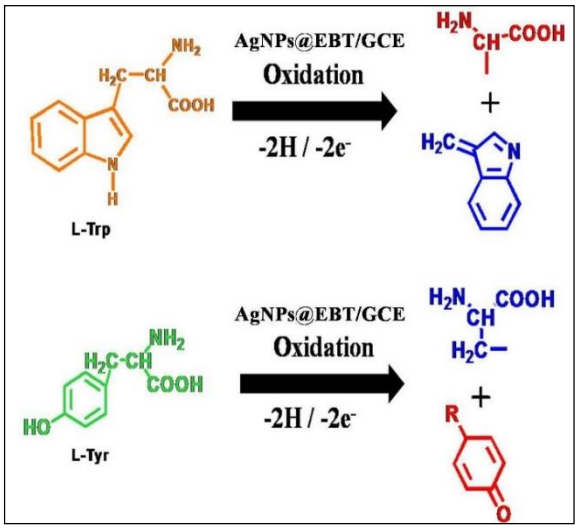

Scheme 2 Electrocatalytic oxidation mechanism of L-Trp and L-Tyr at AgNPs@EBT/GCE

3.8 Effect of Scan Rate

The effect of scan rate on the oxidation peak current of both the L-Trp and L-Tyr at the AgNPs@EBT/GCE was determined and is shown in Fig. 5(C and D). The cyclicvoltammetry (CV) behavior of L-Trp and L-Tyr on AgNPs@EBT/GCE was studied at different scan rates and under similar experimental conditions. The resulting oxidation peak potential and currents were recorded. The oxidation peak current of L-Trp and L-Tyr increases with increasing potential scan rate from 20 mVs^{-1} to 100 mVs^{-1} is shown in Fig. 5(C and D). The correlation coefficients of the above two cases being I_{pa} (µA) = 0.373 mV s^{-1} + 0.0153 (R^2 = 0.9931) and I_{pa} (µA) = 0.021 mVs^{-1}+ 0.25 (R^2 = 0.9751), respectively and are depicted in Fig. 6A (a and b). Moreover, the scan rate study was important to confirm both the diffusion and adsorption controlled reactions. The graph $v^{1/2}$ vs I_{pa} (in Fig. 6B(a and b)) shows the linear relationship in the range 20 mVs^{-1} to 100 mVs^{-1}. In order to verify the diffusion control process, the following equation has been employed: I_{pa} (µA) = 0.334 $v^{1/2}$ (mV/s) $^{1/2}$ + 3.672, R^2 = 0.96751 and I_{pa} (µA) = 0.41 $v^{1/2}$ (mV/s)$^{1/2}$ + 5.325, R^2 = 0.9777 for L-Trp and L-Tyr, respectively. The plot of lnv (mV/s) vs lnI_{pa} (µA) in (Fig. 6C(a and b)) indicates the linear behaviour and also evidences the diffusion controlled reaction [40] for L-Trp and L-Tyr with the values I_{pa} (µA) = 0.05 lnv (mV/s) + 0.534, R^2 = 0.9640 and I_{pa} (µA) = 0.06 lnv (mV/s) + 0.5440, R^2 = 0.9507, respectively. It was found in CV that, both L-Trp and L-Tyr were first adsorbed at the electrode surface and then undergoes irreversible reactions [42, 43].

A positive shift in the peak potential of L-Trp and L-Tyr systems was observed with increase in the scan rate according to Fig. 6D(a and b). The

Cite this Article as: E. Prabakaran, V. Sheela Violet Rani, A. Brabakaran, K. Pandian, D. Jesudurai, A green approach to the synthesis of Eriochrome Black-T capped silver nanoparticles and its electrochemical detection of L-tryptophan and L-tyrosine in blood sample and antibacterial activity, J. Adv. Electrochem. 2(2) (2016) 78–84.

α value can be obtained by plotting E_{pa} vs lnv, a slope of 2.3RT/αnF can be obtained and the αn values was found to be 0.001 and 0.002 for L-Trp and L-Tyr, respectively. The electron transfer rate constant for L-Trp and L-Tyr is calculated and is found to be k_s = 0.53 (cm /s) and k_s = 0.47 (cm/s), respectively [44].

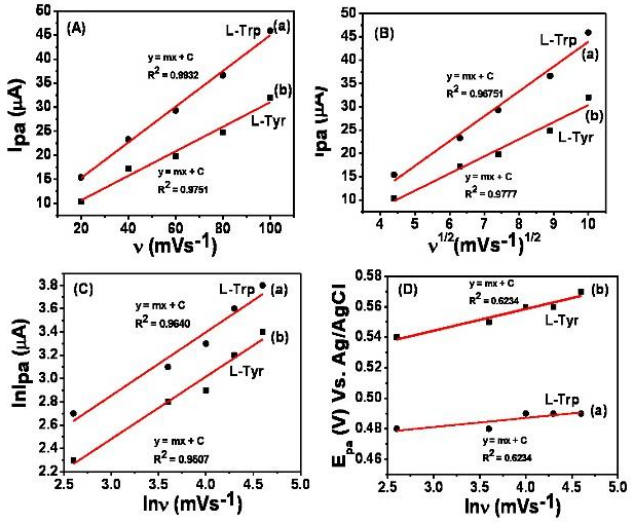

Fig. 6 (A) Calibration plot of I_{pa} (μA) vs. ν (mV / s) for (a) L-Trp and (b) L-Tyr. (B) Calibration plot of I_{pa} (μA) vs. $ν^{1/2}$ (mV / s)$^{1/2}$ for (a) L-Trp and (b) L-Tyr. (C) Calibration plot of lnI_{pa} (μA) vs. lnν (mV / s) for (a) L-Trp and (b) L-Tyr. (D) Calibration plot of E_{pa} (V) vs. lnν (mV / s) for (a) L-Trp and (b) L-Tyr.

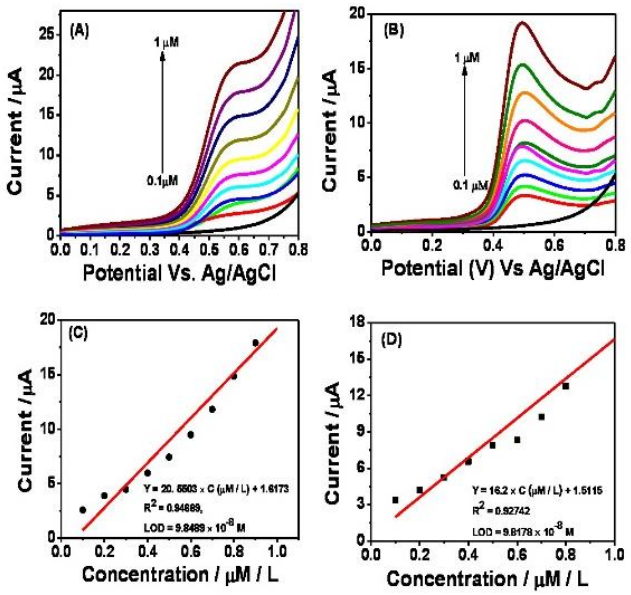

Fig. 7 Linear Sweep Voltammetry responses of L-Trp (A) and L-Tyr (B) observed in 0.1 M PBS on AgNPs@EBT/GCE at a different concentration of 0.1 μM to 1 μM. Calibration plot of I_{pa} vs. C (μM / L) for L-Trp (C) and L-Tyr (D).

3.9 LSV Detection of L-Trp and L-Tyr by using AgNPs@EBT/GCE

The Fig. 7(A and B) depicts the linear sweep voltammetry data for L-Trp and L-Tyr, respectively, recorded at AgNPs@EBT/GCE having the potential of 0 to 0.8 V in 0.1 M PBS (pH 6.0). Upon every addition of L-Trp or L-Tyr into the AgNPs@EBT/GCE system, there is an increase in peak current for each addition. Figure.7 (C & D) shows the corresponding calibration curves for L-Trp and L-Tyr, respectively at the AgNPs@EBT/GCE. The analysis on LSV data delivers the following characteristics: the AgNPs@EBT/GCE displayed high sensitivity (1 μA mM^{-1} and 0.93 μA mM^{-1}), low detection limit (9.848 × 10^{-8} M and 9.817 × 10^{-8} M at S/N = 3), fast response time (5 s) and wide linear range from 0.1× 10^{-6} to 10 × 10^{-5} M (N = 9, R^2 = 0.9468) and 0.1 × 10^{-6} to 0.94 × 10^{-5} M (N = 9, R^2 = 0.9274) for L-Trp and L-Tyr, respectively. The above data from LSV studies and their calibration curves when using AgNPs@EBT/GCE strongly confirms the following advantages. They are: high sensitivity, low detection limit (LOD) and wide linear range of the AgNPs@EBT/GCE for L-Trp and L-Tyr detections. From the LSV studies, it is inferred that the modified AgNPs@EBT/GCE system displays a decrease in surface passivation effects and an increase in electroactivity properties than that of both bare GCE and EBT/GCE. About six parallel determinations were done on using AgNPs@EBT/GCE in order to obtain the RSD value, which is found to be 4.3 %. Furthermore, the analytical performance of the developed L-Trp and L-Tyr sensors was compared with that of other electrochemical sensors [17-14]. The sensor performances with different electrochemical systems are summarized in Table 2.

Table 2 The comparison of electrocatalytic detection of AgNPs@EBT/GCE with other sensors (Analyte L-Trp, L-Tyr)

Electrode	Technique	LOD* (μM)		Linear range (μM)		Ref.
MWCNT/GCE	SWSV[e]	-	0.4	-	2-500	[7]
TiO_2-GR/4-ABSA/GCE[a]	DPV[f]	0.3	-	1-30	-	[8]
MWCNT-CPE[b]	Amp[g]	0.033	-	0.6-9.0	-	[9]
Nafion/TiO_2-graphene/GCE	DPV	0.7	2.3	5-140	10-160	[10]
ERGO/GCE[c]	DPV	0.1	0.2	0.2-40	0.5-80	[11]
Boron-doped diamond	DPV	10	1	20-1000	100-700	[12]
SWCNH/GCE[d]	LSV[h]	0.05	0.4	0.5–50	2-30	[13]
AgNPs/GO/GCE	DPV	0.002	-	0.01-50, 50-800	-	[14]
AgNPs@EBT/GCE	LSV	0.0984	0.0981	0.1-1	0.1 - 0.9	Present Work

*[a]tio2-Graphene/Poly(4-Aminobenzenesulfonic Acid) Composite Film Modified Glassy Carbon Electrode (Tio2-GR/4-ABSA/GCE); [b]multi-Walled Carbon Nanotube Modified Carbon Paste Electrode (MWCNT-CPE); [c]electrochemically Reduced Graphene Oxide Modified Glassy Carbon Electrode (ERGO/GCE); [d]single-Walled Carbon Nanohorns Modified Glassy Carbon Electrode (SWCNH/GCE); *Limit Of Detection (LOD); [e] Square Wave Stripping Voltammetry (SWSV); [f] Difference Pulse Voltammetry (DPV); [g] Amperometry (Amp); [h] Linear Sweep Voltammetry (LSV)*

3.10 Reproducibility and Stability

The reproducibility of the modified AgNPs@EBT/GCE sensor system was tested for about six times by taking an aliquot of L-Trp (100 μL) on each addition and the sensitivity also was determined with a simultaneous current response are presented in Fig. 8(A and B). The relative standard deviation (RSD) is found to be 1.8 %. AgNPs@EBT/GCE appears to show a better stability through oxidation of L-Trp in 100 μL under cyclicvoltammetry as exemplified from the Fig. 8A. The current response towards the oxidation was recorded over a period of 300 min. The AgNPs@EBT/GCE exhibits a slow and gradual decay of the signal with a RSD value of 1.0 % and 4.0 % after 60 min and 300 min, respectively as shown in Fig. 8B. Thus, the electrocatalytic action of the AgNPs@EBT/GCE is maintained over a long period of time and this suggests a fairly good long-term stability of the modified electrode.

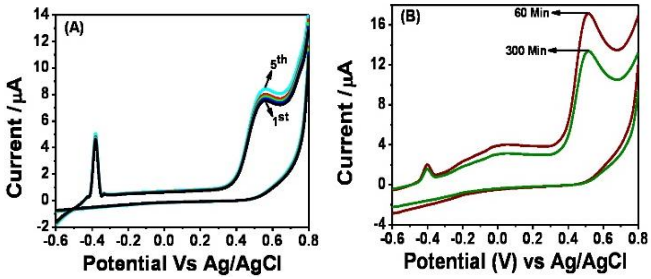

Fig. 8 (A) Cyclicvoltammogram of AgNPs@EBT/GCE in 0.1 M PBS for (1 -5 time) of 1 × 10^{-3} M L-Trp. (B) Current response of the modified AgNPs@EBT/GCE towards 1 × 10^{-3} M of L-Trp over a period of 60 and 300 min.

3.11 Real Samples Analysis

Biologically, the blood contains a number of amino acids and their specific concentration level is detected using the modified AgNPs@EBT/GCE by cyclicvoltammetry method. The following procedure was adopted for the analysis of two samples: 100 times diluted blood samples are mixed with L-Trp solution. The mixture of these two solutions was taken into a 10 mL cuvette in 0.1 M PBS (pH 6.0). About six measurements were done simultaneously on each sample with an average recovery value of 102 % for sample 1 and 96.75 % for sample 2 and the experimental results are given in Table 3.

Table 3 Electrochemical determination of L-Trp and L-Tyr in blood samples (n = 6)

Blood Samples	Compound	Added (μM)	Found (μM)	Recovery (%)	Average (%)
1	L-Trp	10	10.3	106	102
	L-Tyr	10	9.8	98	
2	L-Trp	10	8.7	93.5	96.75
	L-Tyr	10	10	100	

Cite this Article as: E. Prabakaran, V. Sheela Violet Rani, A. Brabakaran, K. Pandian, D. Jesudurai, A green approach to the synthesis of Eriochrome Black-T capped silver nanoparticles and its electrochemical detection of L-tryptophan and L-tyrosine in blood sample and antibacterial activity, J. Adv. Electrochem. 2(2) (2016) 78–84.

3.12 Interference Studies

Various amino acids such as L-alanine, L-glycine and L-arginine etc., are present in human blood samples. But the electrode system AgNPS@EBT/GCE exhibits good sensor properties towards the selective detection of L-Trp and L-Tyr. The electro active system can detect these amino acids even present in very less amount (50 µL). The voltammetric responses of L-Trp and L-Tyr were not affected by the above said amino acids present in blood sample.

3.13 Antibacterial Analysis

The AgNPs@EBT synthesized by green route was employed for the toxicity analysis against gram positive and gram negative pathogenic bacteria [45]. The EBT do not show any inhibition zone and thus its antibacterial effect is not measurable, whereas the EBT containing AgNPs exhibits higher antibacterial effect. The zone of inhibition by AgNPs@EBT was compared against the reference antibiotics drug (ciprofloxacin 5 µg/mL). The present study clearly indicates that the EBT stabilized AgNPs possesses an excellent antibacterial activity against both the gram positive (*Staphylococcus aureus and Streptococcus species*) and gram negative organisms (*Escherichia Coli and Klebsilla species)*.

4. Conclusion

The EBT-capped silver nanoaprticles, AgNPs@EBT was synthesized by a new development and green approach. The AgNPs@EBT was prepared at room temperature when the reactants were exposed to sunlight in a static condition and the nanoparticles were obtained in good yield. An in-depth analysis on UV-Visible and FT-IR spectroscopic data on EBT and AgNPs@EBT indicate the formation of AgNPs@EBT. The PXRD analysis further reinforces the synthesis of crystalline AgNPs@EBT. The synthesized AgNPs@EBT was modified on GCE and employed for the quantitative detection of L-Trp and L-Tyr in blood samples using the Linear Sweep Voltammetry technique in the PBS medium. This sensor system of AgNPs@EBT/GCE exhibits good sensitivity towards the selective determination of L-Trp and L-Tyr in blood samples. The AgNPs@EBT/GCE shows an enhanced electrocatalytic response towards L-Trp and L-Tyr and the lower detection limit (LOD) for L-Trp and L-Tyr is found to be 9.848×10^{-8} M and 9.817×10^{-8} M, respectively. This sensor material displayed good stability during the real sample analysis. The adopted method could extensively be used for the electro-analytical detection of other biosamples. The AgNPs@EBT was also utilized for the successful application of antibacterial studies. From the antibactertial activity studies, it is inferred that the AgNPs containing EBT exhibits excellent bacteriostatic effect against microorganisms.

Acknowledgements

The authors acknowledge the Management, and Department of Chemistry, GKM College of Engineering & Technology (GKMCET), New Perungalathur, Chennai – 600063, India and also thank Dr. M. Prabhu, GKMCET for his help in our work. The authors also acknowledge Indian Institute of Technology, Madras, (IIT-Madras), Chennai-36 and Nanotechnology, University of Madras, Chennai-25, India for providing XRD and FE-SEM and the Antibacterial activity facilities, at the University of Madras, Chennai-25, India.

References

[1] E. Longo, L.S. Cavalcane, D.P. Volanti, A.F. Gouveia, V.M. Longo, J.A. Varela, et al, Direct in situ observation of the electron-driven synthesis of Ag filaments on a-Ag_2WO_4 crystals, Sci. Rep. 3 (2013) 1676-1679.

[2] A. Agazzi, F. De Ponti, R. De Giorgio, S.M. Candura, L. Anselmi, E. Cervio, et al, Review of the implications of dietary tryptophan intake in patients with irritable bowel syndrome and psychiatric disorders, Dig Liver Dis. 35 (2003) 590-595.

[3] A.J. Gelenberg, C.J. Gibson, J.D. Wojcik, Neurotransmitter precursors for the treatment of depression, Psychopharmacol. Bull. 18 (1982) 7-18.

[4] S. Hao, Y. Avraham, O. Bonne, E.M. Berry, Separation-induced body weight loss, impairment in alternation behavior, and autonomic tone: effects of tyrosine, Pharmacol. Biochem. Behav. 68 (2001) 273-281.

[5] G.A. Molnar, Z. Wagner, L. Marko, T. Ko Szegi, M. Mohas, B. Kocsis, et al, Urinary ortho-tyrosine excretion in diabetes mellitus and renal failure: Evidence for hydroxyl radical production, Kidney Int. 68 (2005) 2281- 2287.

[6] M.S. Alaejos, F.J.G. Montelongo, Amperometric biosensors to the determination of vitamins and α-amino acids, Chem. Rev. 104 (2004) 3239–3265.

[7] Q. Xu, S.F. Wang, Electrocatalytic oxidation and direct determination of L-tyrosine by square wave voltammetry at multi-wall carbon nanotubes modified glassy carbon electrodes, Microchim. Acta 151 (2005) 47-52.

[8] C.X. Xu, K.J. Huang, Y. Fan, Z.-W. Wu, J. Li, T. Gan, Simultaneous electrochemical determination of dopamine and tryptophan using a TiO_2-graphene/poly (4-aminobenzenesulfonic acid) composite film based platform, Mater. Sci. Eng. C 32 (2012) 969–974.

[9] T. Thomas, R.J. Mascarenhas, O.J. D'Souza, P. Martis, J. Dalhalle, B.E. Kumara Swamy, Multi-walled carbon nanotube modified carbon paste electrode as a sensor for the amperometric detection of L-tryptophan in biological samples, J. Colloid. Interf. Sci. 402 (2013) 223-229.

[10] Y. Fan, J.H. Liu, H.T. Lu, Q. Zhang, Electrochemistry and voltammetric determination of L-tryptophan and L-tyrosine using a glassy carbon electrode modified with a Nafion/TiO_2-graphene composite film, Microchim. Acta 173 (2011) 241–247.

[11] K.Q. Deng, J.H. Zhou, X.F. Li, Direct electrochemical reduction of graphene oxide and its application to determination of L-tryptophan and L-tyrosine, Colloids Surf B: Biointerf.101 (2013) 183-188.

[12] G.H. Zhao, Y. Qi, Y. Tian, Simultaneous and direct determination of tryptophan and tyrosine at boron-doped diamond electrode, Electroanal. 18 (2006) 830–834.

[13] S. Zhu, J. Zhang, X.E. Zhao, H. Wang, G. Xu, J. You, Electrochemical behavior and voltammetric determination of L-tryptophan and L-tyrosine using a glassy carbon electrode modified with single-walled carbon nanohorns, Microchim. Acta 181 (2014) 445–451.

[14] J. Li, D. Kuang, Y. Feng, F. Zhang, Z. Xu, M. Liu, D. Wang, Green synthesis of silver nanoparticles–graphene oxide nanocomposite and its application in electro-chemical sensing of tryptophan, Biosens. Bioelectron. 42 (2013) 198–206

[15] Y. Huang, X.F. Duanx, Q.Q. Wei, C.M. Liber, Directed assembly of one-dimensional nanostructures into functional network, Sci. 291 (2001) 630-633.

[16] X. Sun, Y. Li, Synthesis and characterization of ion-exchangeable titanate nanotubes, Chem. Eur. J. 9 (2003) 2229–2238.

[17] B.R. Martin, S.K. St Angelo, T.E. Mallouk, Interactions between suspended nanowires and patterned surfaces, Adv. Funct. Mater. 12 (2002) 759–765.

[18] W.L. Barnes, A. Dereux, T.W. Ebbesen, Surface plasmon subwavelength optics, Nature 424 (2003) 824-830.

[19] R. Narayanan, M.A. El-Sayed, Catalysis with transition metal nanoparticles in colloidal solution: nanoparticle shape dependence and stability, J. Phys. Chem. B 109 (2005) 12663-12676.

[20] N.L. Rosi, C.A. Mirkin, Nanostructures in biodiagnostics, Chem. Rev. 105 (2005) 1547-1562.

[21] V.K. Sharma, R.A. Yngard, Y. Lin, Silver nanoparticles: Green synthesis and their antimicrobial activities, Silver nanoparticles: synthesis through chemical methods in solution and biomedical applications, Adv. Colloid Interf. Sci. 145 (2009) 83-96.

[22] S. Shrivastava, T. Bera, A. Roy, G. Singh, P. Ramachandrarao, D. Dash, Characterization of enhanced antibacterial effects of novel silver nanoparticles, Nanotechnol. 18 (2007) 225103-225111.

[23] J.G. Barrasa, J.M. López-de-Luzuriaga, M. Monge, Silver nanoparticles: synthesis through chemical methods in solution and biomedical applications, Cent. Eur. J. Chem. 9 (2011) 7-19.

[24] K.S. Lee, M.A. El-Sayed, Gold and silver nanoparticles in sensing and imaging: sensitivity of plasmon response to size, shape, and metal composition, J. Phys. Chem. B 110 (2006) 19220-19225.

[25] J. Heicklen, Colloid formation and growth, Academic Press, NewYork, 1976.

[26] K.P. Velikov, G.E. Zegers, A.V. Blaaderen, Synthesis and characterization of large colloidal silver particles, Langmuir 19 (2003) 1384-1389.

[27] I. Sondi, D.V. Goia, E. Matijevic, Preparation of highly concentrated stable dispersions of uniform silver nanoparticles, J. Colloid Interf. Sci. 260 (2003) 75-81.

[28] E. Prabakaran, K. Pandian, Amperometric detection of Sudan I in red chili powder samples using Ag nanoparticles decorated graphene oxide modified glassy carbon electrode, Food Chem. 166 (2015) 198-205.

[29] X.P. Tan, Q. Li, Y. Shen, H. Wu, Y. Zhao, J. Yang, Chiral recognition of tyrosine enantiomers based on decreased resonance scattering signals with silver nanoparticles as optical sensor, Chirality 27 (2015) 194–198.

[30] L. Rastogi, J. Arunachalam, Sunlight based irradiation strategy for rapid green synthesis of highly stable silver nanoparticles using aqueous garlic (Allium sativum) extract and their antibacterial potential, Mater. Chem. Phys 129 (2011) 558-563.

[31] Y. Luo, Size-controlled preparation of polyelectrolyte-protected gold nanoparticles by natural sunlight radiation, Mater. Lett. 61 (2007) 2164-2166.

[32] E. Prabakaran, S. Parani, M. Alexander, P. Paulraj, K. Pandian, Synthesis of chitosan oligomer stabilized silver nanorod and its modified glassy carbon electrode for reduction of chlorophenols, J. Nanosci. Lett. 3 (2013) 18-26.

[33] C. Krishnaraj, E.G. Jagan, S. Rajasekar, P. Selvakumar, P.T. Kalaichelvan, N. Mohan, Synthesis of silver nanoparticles using *Acalypha indica* leaf extracts and its antibacterial activity against water borne pathogens, Colloids Surf. B Biointerf. 76 (2010) 50-56.

[34] S. Singha, J.P. Saikia, A.K. Buragohaina, A novel 'green' synthesis of colloidal silver nanoparticles (SNP) using *Dillenia indica* fruit extract, Colloids Surf. B Biointerf. 102 (2013) 83-85.

[35] J. Pulit, M. Banach, Preparation of nanocrystalline silver using gelatin and glucose as stabilizing and reducing agents, respectively, Dig. J. Nanomater. Biostruct. 8 (2013) 787-796.

[36] X. Liu, L. Luo, Y. Ding, Z. Kang, D. Ye, Simultaneous determination of L-cysteine and L-tyrosine using Au-nanoparticles/poly-eriochrome black T film modified glassy carbon electrode, Bioelectrochem. 86 (2012) 38-45.

[37] H.Z.X. Wu, F. Meng, J. Yang, M. Wang, Nucleic acids determination using the complex of eriochrome black T and silver nanoparticles in a resonance light scattering technique, Spectrochim. Acta Part A 78 (2011) 681–686.

[38] X. Zhai, S. Efrima, Reduction of silver ions to a colloid by eriochrome black T, J. Phys. Chem. 100 (1996) 1779-1785.

[39] D. Yogev, D. Rostkier-Edelstein, S. Efrima, Macro emulsions of silver metal liquid-like films, J. Colloid Interf. Sci 147 (1991) 78-87.

Cite this Article as: E. Prabakaran, V. Sheela Violet Rani, A. Brabakaran, K. Pandian, D. Jesudurai, A green approach to the synthesis of Eriochrome Black-T capped silver nanoparticles and its electrochemical detection of L-tryptophan and L-tyrosine in blood sample and antibacterial activity, J. Adv. Electrochem. 2(2) (2016) 78–84.

[40] A. Sarkar, K.A. Kumar, Evaluation of in vitro and in vivo antibacterial activity of dobutamine hydrochloride, J. Med. Microbiol. 21 (2003) 172-178.
[41] R.S. Nicholson, Theory and application of cyclic voltammetry for measurement of electrode reaction kinetics, Anal. Chem. 37 (1965) 1351-1355.
[42] A.J. Bard, L.R. Faulkner, Electrochemical methods. Fundamentals and applications, 2nd Ed., John Wiley & Sons, New York, 2000.
[43] E. Laviron, General expression of the linear potential sweep voltammogram in the case of diffusionless electrochemical systems, J. Electroanal. Chem. 101 (1979) 19-28.
[44] E. Laviron, The use of linear potential sweep voltammetry and of a.c. voltammetry for the study of the surface electrochemical reaction of strongly adsorbed systems and of redox modified electrodes, J. Electroanal. Chem. 100 (1979) 263-270.
[45] M. Zargar, A.A. Hamid, F.B. Bakar, M.N. Shamsudin, K. Shameli, F. Jahanshiri, F. Farahani, Green synthesis and antibacterial effect of silver nanoparticles using Vitex Negundo L, Molecules 16 (2011) 6667- 6676.

Cite this Article as: E. Prabakaran, V. Sheela Violet Rani, A. Brabakaran, K. Pandian, D. Jesudurai, A green approach to the synthesis of Eriochrome Black-T capped silver nanoparticles and its electrochemical detection of L-tryptophan and L-tyrosine in blood sample and antibacterial activity, J. Adv. Electrochem. 2(2) (2016) 78–84.